VOL. 11, NO. 22, NOVEMBER 2016 ISSN 1819-6608
ARPN Journal of Engineering and Applied Sciences

www.arpnjournals.com

AN ANALYTICAL INVESTIGATION OF THE GROOVED JOURNAL BEARING'S PERFORMANCE WITH SLIP/ NO-SLIP TEXTURE BEARING

K. M. Faez, S. Hamdavi, H. H. Ya and T V V L N Rao
Department of Mechanical Engineering, Universiti Teknologi Petronas, Bandar Seri Iskandar, Perak, Malaysia
E-Mail: kumuhammadfaez@gmail.com

ABSTRACT

The hydrodynamic journal bearings are widely used in different industries for high speed and high loads. Meanwhile, its performance and reliability is a big concern. Surface texturing is a suitable and an accepted way to improve its performance. In this paper, the altered Reynolds equation is done to calculate the load carrying capacity for convergent long journal bearings with slip and no-slip pattern. Furthermore, to investigate the load carrying capacity performance some defined parameters has changed to study their changes towards the performance of journal bearing, e.g. number of slip regions, depth of grooved, etc. From the results, it can be seen that increasing the slip and no-slip region length gives a promising impact towards the load carrying capacity for convergent long journal bearing.

Keywords: surface texturing; slip/no-slip region; load carrying capacity; hydrodynamic journal bearings.

INTRODUCTION

In hydrodynamic lubrication contacts, partial texture and partial slip gives a lot of interest as it improves the bearing performance. The configuration of partial texture and partial slip at the surfaces is efficient to improve the bearing performance. In addition, these configurations have capabilities to support higher load capacity thus increase the bearing performance in real-life usage.

Textured hydrodynamic lubricated contacts has provided a great interest as the texturing bearing surfaces concept has led to increased load capacity or reduced the friction of the relative motion. The load carrying capacity for different roughness profile was studied by Tonder [1], he showed that applying the roughness improves the load carrying capacity. At the same time, Etsion *et al.* [2] presents of ability of micro-dimples at thrust bearings with the same improvement as well. Furthermore, Fowel *et al.* [3] explored how the textured profile can influence the performance of slider bearing based on parameters of the geometry's surface texture such as the textures number, depth, width, and its location. Cupillard *et al.* [4] proved that the texture in the converging gap of journal bearing has increase its hydrodynamic performance. Tauviqirrahman *et al.* [5] is then did some changes of the Reynolds equation according to variations of surface pattern such as texturing and slip. From the modification, it is proven that partial texturing at the surface provides better improvements compare to full texturing.

Another approach regarding the Reynolds equation will give the boundary conditions of the no-slip lubrication towards the two contacts at a relative motion. Craig *et al.* [6], Zhu and Garnick [7], and Spikes [8] studied that the presents of slip is due to the even and microgeometrical environments. Wu *et al.* [9] studied the hydrodynamics properties based on the slip influence in the journal bearing. Rao *et al.* [10] studied the effect of partial slip conditions towards the grooved concentric of journal bearing in load capacity and friction coefficient. Meanwhile, Salant and Fortier [11] described the numerical analysis for the combination of slip and/or no-slip configuration for bearing surface by using modified slip length results a higher load capacity and lower friction. Hamdavi *et al.* [12] also proved that having a partial texture surface at the infinite hydrodynamic journal bearing produced significant effect and performance based on the calculation on the oil film pressure and the comparison in the distribution of pressure with the plain surface.

In this paper, partial texture with slip and no-slip design is a major consideration to investigate the behavior of the load carrying capacity. One-dimensional analysis of stationary journal bearing is considered, in which involves some part in the slip texture of journal bearing. In addition, plain surface and complete texturing gives negative impact towards bearing performance as compare to partial texturing. The partially textured region consists of land, no-slip surfaces together with slip surfaces at the grooved region. Reynolds equation is altered according to partial texture configuration has acquired for this approach. The boundary conditions of the configuration are applied to determine the distribution of dimensionless pressure in the journal bearing. From the results obtained, the load capacity is calculated and obtained from the oil flow volume equation. The overall change in load capacity is analyzed through the sets of figures.

METHOD OF ANALYSIS

The journal bearing is analyzed by showing an alternate land and recess region, in which the land no-slip surface at the land and the slip surface at the grooved region as shown in Figure-1. The angular length for the recess with slip region is known as $\theta_{1,2} - \theta_{1,1} = ... = \theta_{n,2} - \theta_{n,1} = \theta_s$, meanwhile the angular length of the land with no-slip region is noted as $\theta_{1,3} - \theta_{1,2} = ... = \theta_{n,3} - \theta_{n,2} = \theta_n$. θ_t is known as the textured length. This analysis is based on the Reynolds

boundary conditions. At the end of partially textured surface, the groove in which a slip region is noted as $\theta_g - \theta_t$.

From the Figure-1, the dimensionless thickness of the film at the recess and groove regions is expressed as $H + H_r$ and $H' = H + H_g$, in which

$$H = (1 + \varepsilon \cos \theta) \quad (1)$$

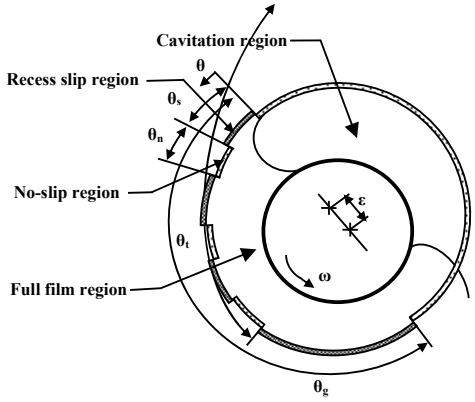

Figure-1. Geometry of grooved, partially textured through slip/no-slip configuration of journal bearing.

The slip and no-slip for regions *s* has its boundary conditions in which stated below respectively.

$$P|_{\theta=0} = 0, P|_{\theta=\theta_{1,2}} = P_{1,2} \text{ and } P|_{\theta=\theta_{1,3}} = P_{1,3} \quad (2)$$

The modified Reynolds equation for partial slip surface in dimensionless form is;

$$\frac{d}{d\theta}\left[\frac{H^3(H+4A)}{12(H+A)}\frac{dp}{d\theta}\right] = \frac{1}{2}\frac{d}{d\theta}\left[\frac{H(H+2A)}{(H+A)}\right] \quad (3)$$

Integrating Equation. (3) gives the profiles of dimensionless pressure of slip and no-slip region as

$$\frac{dP}{d\theta}\left(0 \le \theta \le \theta_{1,2}\right) = \frac{6(H'+2A)}{H'^2(H'+4A)} - \frac{12(H'+A)Q}{H'^3(H'+4A)} \quad (4)$$

$$\frac{dP}{d\theta}\left(\theta_{1,2} \le \theta \le \theta_{1,3}\right) = \frac{6}{H^2} - \frac{12Q}{H^3} \quad (5)$$

Integrating both Equation. (4) and (5) together with the substitution of the boundary conditions in Equation. (2) gives the profiles of dimensionless pressure of slip and no-slip for region *s* as

$$P_1\left(0 \le \theta \le \theta_{1,2}\right) = P|_{\theta=0} + 6\int_0^{\theta_{1,2}} \frac{(H'+2A)}{H'^2(H'+4A)}d\theta - 12Q\int_0^{\theta_{1,2}} \frac{(H'+A)}{H'^3(H'+4A)}d\theta \quad (6)$$

$$P_2\left(\theta_2 \le \theta \le \theta_3\right) = P|_{\theta=1,2} + 6\int_{\theta_{1,2}}^{\theta_{1,3}} \frac{1}{H^2}d\theta - 12Q\int_{\theta_{1,2}}^{\theta_{1,3}} \frac{1}{H^3}d\theta \quad (7)$$

The boundary conditions based on Reynolds equation for dimensionless pressure is substituted and simplified using the pressure obtained previously, in which yield the results in flow volume, Q as

$$Q = \frac{\sum_4^n\left(\int_{\theta_{i,1}}^{\theta_{i,2}} \frac{(H'+2A)}{H'^2(H'+4A)}d\theta + \int_{\theta_{i,2}}^{\theta_{i,3}} \frac{1}{H^2}d\theta + \right) + \int_{\theta_t}^{\theta_g} \frac{(H'+2A)}{H'^2(H'+4A)}d\theta}{\sum_4^n\left(\int_{\theta_{i,1}}^{\theta_{i,2}} \frac{2(H'+A)}{H'^3(H'+4A)}d\theta + \int_{\theta_{i,2}}^{\theta_{i,3}} \frac{2}{H^3}d\theta + \right) + \int_{\theta_t}^{\theta_g} \frac{2(H'+2A)}{H'^3(H'+4A)}d\theta} \quad (8)$$

The dimensionless pressure throughout and perpendicular to the center line is integrate and the result gives the load capacity in terms of radial and tangential, in dimensionless form as shown in Equation. (9) and (10);

$$W_\varepsilon = -\left[\int_{\theta_{i,1}}^{\theta_{i,2}} P_1 \cos\theta\, d\theta + \int_{\theta_{i,2}}^{\theta_{i,3}} P_2 \cos\theta\, d\theta + \int_{\theta_{i,3}}^{\theta_{i,4}} P_3 \cos\theta\, d\theta + \ldots + \int_{\theta_t}^{\theta_g} P_7 \cos\theta\, d\theta\right] \quad (9)$$

$$W_\phi = \left[\int_{\theta_{i,1}}^{\theta_{i,2}} P_1 \sin\theta\, d\theta + \int_{\theta_{i,2}}^{\theta_{i,3}} P_2 \sin\theta\, d\theta + \int_{\theta_{i,3}}^{\theta_{i,4}} P_3 \sin\theta\, d\theta + \ldots + \int_{\theta_t}^{\theta_g} P_7 \sin\theta\, d\theta\right] \quad (10)$$

Thus, the dimensionless load capacity is computed as;

$$W = \sqrt{W_\varepsilon^2 + W_\phi^2} \quad (11)$$

RESULTS AND DISCUSSIONS

To examine the performance of load carrying capacity in grooved journal bearing with pattern of slip and no-slip, some parameters and regions with slip and no-slip, as well as grooved or no-grooved portion should be defined and considered. These parameters are; (A) is the dimensionless slip coefficient with its magnitude is one in the slip region and zero in the no-slip regions; the eccentricity ratio (ε) ranged from 0.2 to 0.8, by increments of 0.2; the dimensionless groove depth (H_g) equals to 1, 2, 3 and 4; (θ_t) is the length for slip region which has the values of 40°, 80°, 120° and 160°; (θ_g) is the angular length for no-slip region defined on the surface of bearing; the ratio of slip to no-slip region is defined by (γ) equals to, 0.2, 0.4, 0.6 and 0.8 and finally; (n) = 2, 4, 6 and 8 is the number of slip regions.

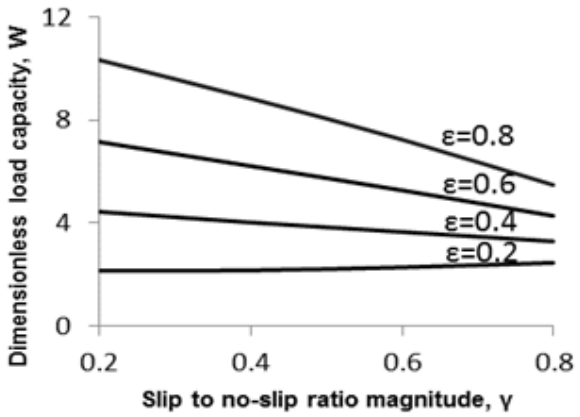

Figure-2(a). Dimensionless load capacity with slip to no-slip ratio at $\theta_t = 120^\circ$, $\theta_g = 180^\circ$, n=4, $H_g = 1$, A = 1.

Figure-2(a) represents how the dimensionless load capacity, influenced by changes in the slip to no-slip ratio (γ) magnitude. The lowest value of the load carrying capacity is observed when the eccentricity ratio defined as ε = 0.2, which can hardly make an increase in the magnitude of load carrying capacity. Once the eccentricity ratio increased from 0.2 to 0.8, the magnitude of load carrying capacity, takes higher values for any range of slip to no-slip ratio range. However, when the value of slip to no-slip ratio goes up, the magnitudes of load carrying capacity tend to decline from their initial values at γ = 0.2 to γ = 0.8. The rate of declining in trend of load carrying capacity is much higher at ε = 0.8 compare to ε = 0.2.

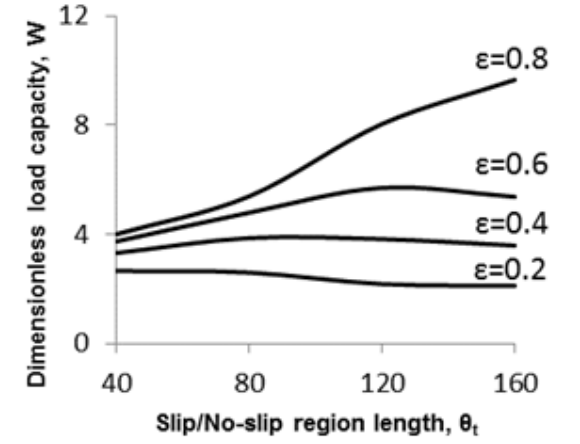

Figure-2(b). Dimensionless load capacity with slip/no-slip region length at $\theta_g = 180^\circ$, n=4, γ = 0.5, $H_g = 1$, A = 1.

In the Figure-2(b), it can clearly be seen that the magnitude of the load carrying capacity has different behaviour when the slip/no-slip region length θ_t, changes from 40° to 160°. The load magnitude rises dramatically from its initial value of almost 4 to the final value of approximately 9, when the eccentricity ratio is ε = 0.8. On the other hand, for lowest eccentricity ratio ε = 0.2, gives this impression that even by increasing in the length of slip and no-slip region, the magnitude of load carrying capacity does not change positively but decreases to the lesser magnitudes than its first value.

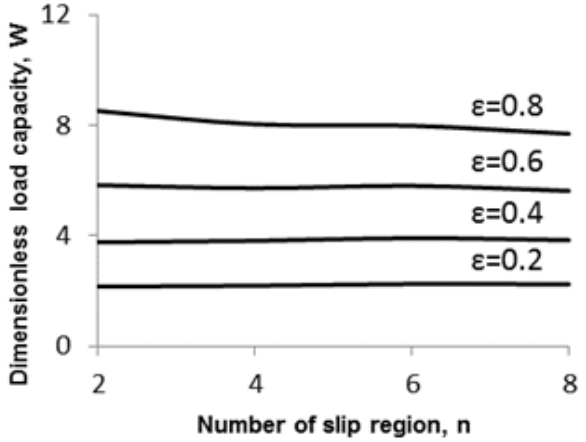

Figure-2(c). Dimensionless load capacity with number of slip region at $\theta_t=120^\circ$, $\theta_g=180^\circ$, γ = 0.5, $H_g=1$, A=1

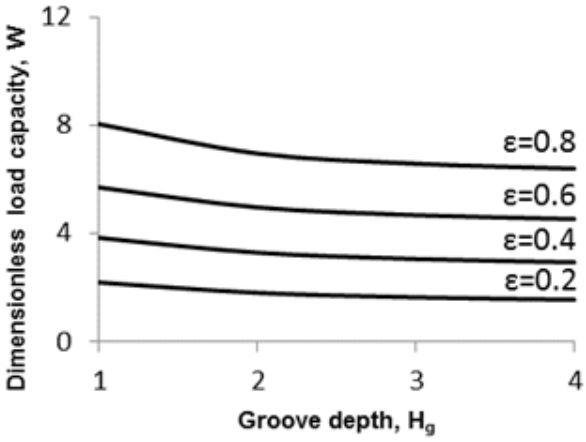

Figure-2(d). Dimensionless load capacity with groove depth at $\theta_t=120^\circ$, $\theta_g=180^\circ$, n=4, γ=0.5, A=1.

For Figure-2(c) and (d), the trends of change in the magnitudes of the load carrying capacity are considered. The load carrying capacity has higher values by increase in the magnitude of eccentricity ratio, by the reason of wedge action in the convergent area between rotating shaft and bearing sleeve. Increasing in groove depth, H_g cannot either keep the value of load carrying capacity stable or makes any improvement. Same results can be inferred from Figure-2(c); number of slip region, n does not have any remarkable influence on the value of load carrying capacity at low eccentricity ratio of 0.2. on the higher eccentricity ratios, the magnitudes of load carrying capacity tends to goes down, by increase in the number of slip region.

CONCLUSIONS

Recent study investigates the change on the dimensionless load carrying capacity for grooved journal bearing with slip and no-slip pattern configuration. Based on the analysis made, it can be deduced that the conclusions for this research are:

- At the eccentricity ratio of 0.8, the increase in the slip ratio magnitude (γ) and dimensionless groove depth (H_g) reduces the dimensionless load carrying capacity.
- At the same eccentricity ratio of 0.8 with similar configuration, once the slip and no slip region length increases, the dimensionless load carrying capacity will increase.
- Increasing the number of slip region, n doesn't provide any significant change towards the dimensionless load carrying capacity.

The analysis of the hydrodynamic grooved journal bearing is studied by applying a newly modified classical Reynolds equation and considering the slip and no-slip region pattern on the grooved bearing surface.

ACKNOWLEDGEMENT

The authors highly appreciate the Ministry of Higher Education (FRGS-MOHE) Malaysia for their support for this research work which is under the grant of Fundamental Research Grant Scheme "FRGS-0153AB-K49".

REFERENCES

[1] Tonder, K., Inlet roughness tribodevices dynamic coefficients and leakage. Tribology International, 2001. 34: p. 847-852.

[2] Etsion, I., Halperin, G. Brizmer, V. and Kligerman, Y. Experimental investigation of laser surface textured parallel thrust bearings. Tribology Letters, 2003. 17(02).

[3] Fowell, M., Olver, A. V., Gosman, A. D., Spikes, H. A. and Pegg, I. Entrainment and Inlet Suction: Two Mechanisms of Hydrodynamic Lubrication in Textured Bearings. Journal of Tribology, 2007. 129(2): p. 336.

[4] Cupillard S., Cervantes M.J. and Glavatskih S., Pressure buildup mechanism in a textured inlet of a hydrodynamic contact. Journal of Tribology, 2008. 130(2): p. 021701.

[5] Tauviqirrahman M., Ismail R., Jamari J. and Schipper D. J., A study of surface texturing and boundary slip on improving the load support of lubricated parallel sliding contacts. Acta mechanica, 2013. 224(2): p. 365-381.

[6] Craig, V.S., C. Neto and D.R. Williams, Shear-dependent boundary slip in an aqueous Newtonian liquid. Physical review letters, 2001. 87(5): p. 054504.

[7] Zhu, Y. and S. Granick, Limits of the hydrodynamic no-slip boundary condition. Physical review letters, 2002. 88(10): p. 106102.

[8] Spikes, H.A., The half-wetted bearing. Part 1: extended Reynolds equation. Proceedings of the Institution of Mechanical Engineers, Part J: Journal of Engineering Tribology, 2003. 217(1): p. 1-14.

[9] Wu, C.W., Ma, G. J., Zhou, P. and Wu, C. D., Low Friction and High Load Support Capacity of Slider Bearing With a Mixed Slip Surface. Journal of Tribology, 2006. 128(4): p. 904.

[10] Rao, T., Rani, A., Nagarajan, T. and Hashim, F., Analysis of Grooved Journal Bearing with Partial Slip Surface. Paper presented at the Proceedings of Regional Tribology Conference 2011: RTC2011.

[11] Fortier, A.E. and R.F. Salant, Numerical Analysis of a Journal Bearing With a Heterogeneous Slip/No-Slip Surface. Journal of Tribology, 2005. 127(4): p. 820.

[12] Hamdavi, S., H. Ya, and T. Rao, Effect of Surface Texturing on Hydrodynamic Performance of Journal Bearings. ARPN Journal of Engineering and Applied Sciences, 2016. 11(01): p. 172-176.